

1 Transformation kinetics of burnt lime in freshwater and sea water

2
3 Harald Justnes^{1,2}, Carlos Escudero-Oñate³, Øyvind Aaberg Garmo³ and Martin
4 Mengede⁴.

5
6 ¹SINTEF Community, Høgskoleringen 7b, 7034 Trondheim, Norway

7 ²NTNU, Faculty of Natural Sciences, Sem Sælandsvei 12, 7034 Trondheim, Norway

8 ³Norwegian Institute for Water Research (NIVA), Gaustadalléen 21, 0349 Oslo,
9 Norway

10 ⁴Franzefoss Minerals AS, Olav Ingstads vei 5, 1309 Rud, Norway

12 Abstract

13 The reaction kinetics of burnt lime (CaO) in contact with sea water has been elucidated
14 and compared to its behaviour in fresh water. In the first minutes of contact between burnt
15 lime and water, it "slaked" as CaO reacted with water to yield calcium hydroxide
16 (Ca(OH)₂). Subsequently, calcium hydroxide reacted with magnesium, sulphate and
17 carbonate from the sea water to yield magnesium hydroxide (Mg(OH)₂), calcium sulphate
18 dihydrate (gypsum, CaSO₄·2H₂O) and calcium carbonate (CaCO₃), respectively. In a
19 closed system of 1% CaO in natural sea water (where the supply of sulphate, magnesium
20 and carbonate is limited), more than 90% reacted within the first 5 hours. It is foreseen
21 that in an open system, like a marine fjord, it will react even faster. The pH 8 of sea water
22 close to the CaO particle surface will immediately increase to a theoretical value of about
23 12.5 but will, in an open system with large excess of sea water, rapidly fall back to pH
24 10.5 being equilibrium pH of magnesium hydroxide. This is further reduced to < 9 due to
25 the common ion effect of dissolved magnesium in sea water and then be diluted to the sea
26 water background pH, about 8. Field test dosing CaO particles to sea water showed that
27 the pH of water between the particles stayed around 8.

28 **Keywords:** Calcium oxide, calcium hydroxide, kinetics, lime, magnesium hydroxide, sea
29 water

30 1 INTRODUCTION

31 1.1 Applications of burnt lime in sea water

32 Calcium oxide (CaO) also known as burnt lime, is being considered as a possible
33 treatment to reduce the negative impact of sea urchins on tare forests in northern coastal
34 waters and blue-green algal blooms in the surrounding of fish-farms (monoculture) [1, 2].
35 The treatment involves a rapid suspension of burnt lime in sea water and immediate
36 discharge into the marine environment. Hence, it becomes of paramount importance to
37 know how CaO particles behaves in contact with sea water and how this substance
38 modifies the water chemistry.

39 The aim of this treatment is to increase tare growth and population density. This would
40 provide a habitat for many species and will increase the biodiversity of the marine
41 environment.

42 On a longer term one can imagine harvesting of high-quality sea urchins for the food
43 market as well as a preparedness plan to treat blue-green algal blooms for the same
44 market. In a wider perspective lime can be used to capture CO₂ in sea water as an
45 environmental remediation. However, designing an efficient treatment strategy to tackle
46 the variable conditions expected in the sea requires increased understanding of the
47 reaction kinetics of CaO in sea water.

48 The burnt lime treatment is usually performed by spraying a suspension of CaO particles
49 directly at the surface of the sea and all these particles will interfere with each other in
50 their microenvironment until the gradual dilution is so great that they can be considered
51 as single particles. For instance, the treatment in practice consists of pumping a slurry of
52 100 kg burnt lime (0.2-0.8 mm diameter) dispersed in 600 litres of sea water onto the
53 surface. This provides an initial CaO concentration in the slurry of 167 g/l, that is taken
54 as a starting point. Assuming that the average particle diameter is 0.5 mm and that they
55 are spherical, will the volume of the particle be $\frac{4}{3}\pi r^3$ or 0.0654 mm³. Light-burnt lime
56 (burnt at 1060°C) has a typical particle density [3] of $\rho_p = 2 \text{ g/cm}^3$. The particle is porous
57 since CaO has solid density $\rho_s = 3.35 \text{ g/cm}^3$; porosity = $(1 - \rho_p/\rho_s) \cdot 100\text{vol}\% = 40 \text{ vol}\%$,
58 which is also what Wuhrer [4] found. This gives then an outer volume of light burnt lime
59 83.5 mm³ or in other words about 1275 particles per ml. These particles will however
60 immediately react with water as discussed in the next section about reaction with fresh
61 water. The reaction with fresh water is evaluated first in order to illustrate the difference
62 to sea water in the section thereafter.

63

64 1.2 Chemistry of burnt lime (CaO) in fresh water

65 Burnt lime reacts violently with water to produce calcium hydroxide (so called slaked
66 lime) according to the reaction below



68 The reaction in Eq. 1 releases a heat of $Q = 1160 \text{ J/g CaO}$. The heat capacity of water is
69 $c = 4.18 \text{ kJ/kg}\cdot\text{K}$. The increase in temperature of a mass (m) of water due to the reaction
70 in Eq. 1 can be calculated by the formula in Eq. 2;

$$71 \Delta T = Q/c \cdot m \quad (2)$$

72 Using the same concentration of particles as in the preceding section (167 g/l) and a
 73 density of water of 1000 g/l, one find that the water will be heated $\Delta T = 167 \text{ g} \cdot 1.160$
 74 $\text{kJ/g} / (4.18 \text{ kJ/kg}\cdot\text{K} \cdot 1 \text{ kg}) = 46 \text{ K} = 46 \text{ }^\circ\text{C}$. This temperature increase is for a closed
 75 system (adiabatic, without heat loss) and 100% hydration of the burnt lime particles and
 76 will be proportional less for decreasing fractions of reaction. The temperature increase as
 77 a function of burnt lime dosage and fraction of hydration is given in Table 1 as an
 78 illustration.

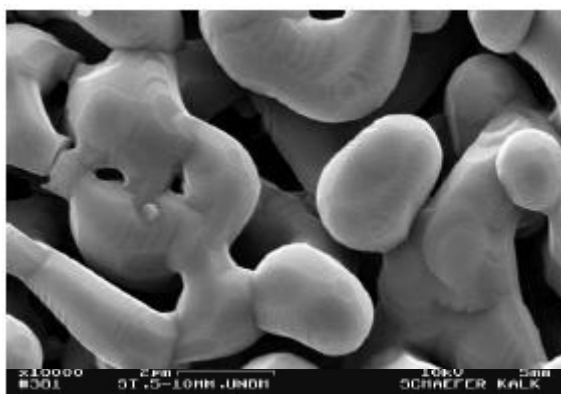
79

80 **Table 1-** Temperature increase (ΔT ; $^\circ\text{C}$) in water as function of dosage of burnt lime and
 81 its hydration fraction as calculated from Eqs. 1 and 2.

Dosage \rightarrow /Hydration fraction \downarrow	200 g/l	150 g/l	100 g/l	50 g/l
0.2	11	8	6	3
0.4	22	17	11	6
0.6	33	25	17	8
0.8	44	33	22	11
1.0	56	42	28	14

82

83 A light-burnt lime particle is not massive, but porous as shown in Fig. 1 [5].



84

85 **Figure 1** – An electron microscopy image of the pore walls of an unhydrated light-burnt
 86 lime particle [5].

87

88 When the lime particle meets water, this will be sucked into the pores and react
 89 immediately to calcium hydroxide while the pore water temperature will increase rapidly
 90 to above the boiling point since there is a small amount of water relative to the CaO of
 91 the pore wall. If the precipitated calcium hydroxide has blocked the pore (Eq. 1 doubles
 92 the volume of solid matter) the particle will disintegrate due to the thermal expansion of
 93 the remaining water and/or its vapor pressure. The reaction can be described as chaotic
 94 and will not be less chaotic when components from sea water interfere as described in
 95 next section. Calcium hydroxide has limited solubility and the solubility actually
 96 decreases with increasing temperature as shown in Eq.3 (calculated from tabular data [6]),
 97 an anomaly compared to most other compounds. The reaction rate of CaO, on the other
 98 hand, increases with increasing temperature and the degree of reaction for a light-burnt

99 lime particle may reach 80% after 1 hour under isothermal conditions, but after < 5
 100 minutes under adiabatic conditions (time to reach 60°C according to EN459-2) depending
 101 on the fineness of the burnt lime.

$$102 \text{ Solubility of Ca(OH)}_2 \text{ (g/l)} = -0.0117 \cdot T \text{ (}^\circ\text{C)} + 1.924 \text{ with } r^2 = 0.9954 \quad (3)$$

103 In order to calculate the pH of burnt lime slaked in distilled water, one can use the
 104 solubility of 1.63 g/l at 25°C (from Eq. 3) knowing that calcium hydroxide dissociates
 105 as written in Eq. 4;



107 where the concentrations of ions in brackets are expressed in mol/L. According to Eq. 4
 108 the concentration of hydroxyl ions is twice that of the dissolved calcium hydroxide;

$$109 [\text{OH}^-] = 2 \cdot [\text{Ca}^{2+}] = 2 \cdot [\text{Ca(OH)}_2] \quad (5)$$

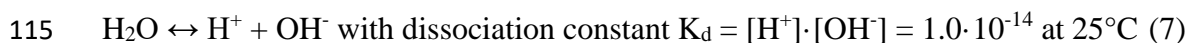
110 since $M_w(\text{Ca(OH)}_2) = 74.08 \text{ g/mol}$,

$$111 [\text{OH}^-] = 2 \cdot 1.63 \text{ g/l} / 74.08 \text{ g/mol} = 0.04405 \text{ mol/l}$$

112 The relation between $[\text{OH}^-]$ and pH at 25°C is;

$$113 \text{ pH} = -\log [\text{H}^+] = 14.00 + \log [\text{OH}^-] \quad (6)$$

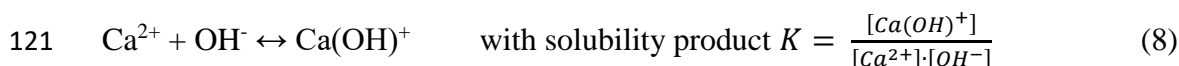
114 since



116 $\text{pH} = -\log [\text{H}^+] = 7$ for neutral water since $[\text{H}^+] = [\text{OH}^-]$ and $[\text{H}^+] = \sqrt{(1.0 \cdot 10^{-14})}$.

117 $[\text{OH}^-] = 0.04405 \text{ M}$ for dissolved calcium hydroxide gives then $\text{pH} = 12.64$ for a solubility
 118 of 1.63 g/l at 25°C.

119 pH will be a bit lower than this as dissolved calcium hydroxide is not completely
 120 dissociated and species like CaOH^+ exists;



122 The geochemical data program GEMS (gems.web.psi.ch) [7, 8] with PSI-GEMS
 123 thermodynamic data base for aqueous species and solids [9] minimizes Gibbs free energy
 124 and gives the following composition of a saturated solution of calcium hydroxide at 25°C:

$$125 [\text{Ca}^{+2}] = 0.016370 \text{ M or } 0.65611 \text{ g/l}$$

$$126 [\text{CaOH}^+] = 0.004265 \text{ M or } 0.24345 \text{ g/l}$$

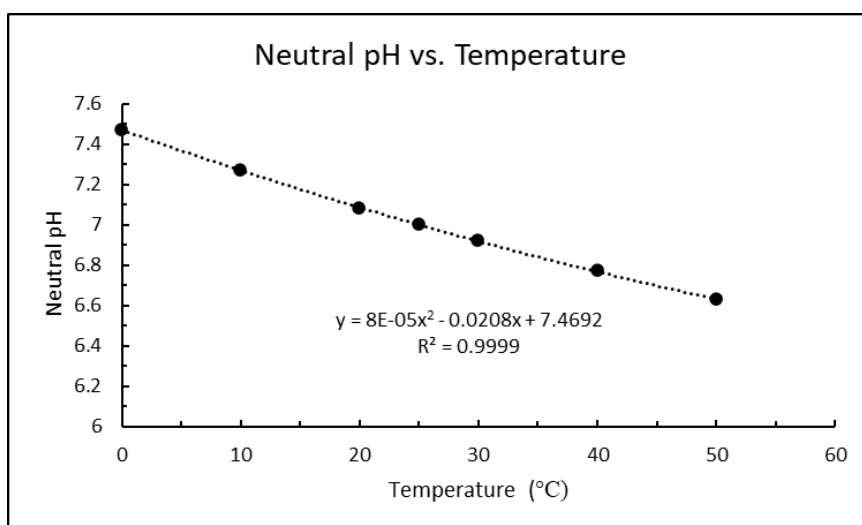
$$127 [\text{OH}^-] = 0.037006 \text{ M or } 0.62910 \text{ g/l}$$

$$128 \text{ pH} = 12.48$$

129 This gives an amount of dissolved calcium hydroxide of 1.53 g/l instead of the 1.63 g/l
 130 obtained through Eq. 3, which explains the difference in calculated pH together with the
 131 presence of the species CaOH^+ . Due to this species the pH as measured by a pH-meter
 132 will be lower than the corresponding amount of dissolved calcium hydroxide; $\text{pH} = 12.62$
 133 for 1.53 g/l dissolved Ca(OH)_2 , which would have been the result if the solution was

134 titrated rather than measured by a pH-meter. The proceeding evaluations will nevertheless
 135 be based on the solubility from Eq. 3 (1.63 g/l resulting in pH = 12.64) and ignore the
 136 presence of species like CaOH^+ since it will react with the different species in sea water
 137 as if it was separated as Ca^{2+} and OH^- .

138 Another complicating factor for correct pH is that the self-dissociation of water in Eq. 7
 139 increases with increasing temperature as temperature is just a measure of molecular
 140 movement. The pH reference value of 14 will then increase with decreasing temperature,
 141 or pH of neutral water will decrease with increasing temperature as plotted in Fig. 2.
 142 Neutral pH at 5 and 15°C would be 7.37 and 7.18, respectively, which corresponds to
 143 reference values of 14.74 and 14.36 (rather than 14.00 in Eq. 7) unless the pH-meter is
 144 correcting for temperature.



145

146 **Figure 2** – pH for neutral water as a function of temperature in the range 0-50°C plotted
 147 from a table in [10].

148 The pH in a suspension of calcium hydroxide will further increase with decreasing
 149 temperature since the solubility of calcium hydroxide increases as shown by Eq. 3.

150 Consider distilled water equilibrating with natural air containing 400 ppm or 0.04 vol%
 151 carbon dioxide. The CO_2 can partly be dissolved as the molecule or react with water to
 152 hydrogen carbonate (so called carbonic acid):

153 $\text{CO}_2 + \text{H}_2\text{O} \leftrightarrow \text{H}_2\text{CO}_3$ with hydration product $K_h = \frac{[\text{H}_2\text{CO}_3]}{[\text{CO}_2(\text{aq})]} = 1.7 \cdot 10^{-3}$ at 25°C (9)

154 The main component of dissolved CO_2 will be molecular $\text{CO}_2(\text{aq})$, since K_h is so small
 155 that the concentration of H_2CO_3 would be negligible and do not influence pH (i.e. \log
 156 $[\text{H}^+]$). The total solubility of CO_2 at 100 kPa CO_2 pressure (about 1 atm) and 25°C is 1.45
 157 g/l.

158 Hydrogen carbonate dissociates according to 2 sequential steps:

159 $\text{H}_2\text{CO}_3 \leftrightarrow \text{H}^+ + \text{HCO}_3^-$ with dissociation constant $K_{a1} = \frac{[\text{HCO}_3^-] \cdot [\text{H}^+]}{[\text{H}_2\text{CO}_3]} = 2.5 \cdot 10^{-4}$ at
 160 25°C (10)

161 $\text{HCO}_3^- \leftrightarrow \text{H}^+ + \text{CO}_3^{2-}$ with dissociation constant $K_{a2} = \frac{[\text{CO}_3^{2-}][\text{H}^+]}{[\text{HCO}_3^-]} = 4.69 \cdot 10^{-11}$ at
 162 25°C (11)

163 The distribution of the different species for CO_2 dissolved in water as a function of pH is
 164 shown in Fig. 3. The solubility of CO_2 is proportional to the partial pressure of carbon
 165 dioxide as shown in Eq. 12 and increases with decreasing pressure as plotted in Fig. 4

166 $[\text{CO}_2] = k \cdot P(\text{CO}_2)$ (12)

167 For two different pressures Eq. 12 can be reformulated to

168 $k = \frac{[\text{CO}_2]_1}{P_1(\text{CO}_2)} = \frac{[\text{CO}_2]_2}{P_2(\text{CO}_2)}$ og at $[\text{CO}_2]_2 = \frac{P_2(\text{CO}_2)}{P_1(\text{CO}_2)} \cdot [\text{CO}_2]_1$ (13)

169 Fig. 3 shows that at 15°C and $P_1(\text{CO}_2) = 1$ atm the concentration of carbon dioxide is
 170 $[\text{CO}_2]_1 = 2$ g/l or 45.45 mM. If k is constant over the whole pressure range, the solubility
 171 at $P_2(\text{CO}_2) = 0.04$ atm will be $[\text{CO}_2]_2 = 0.08$ g/l or 1.82 mM.

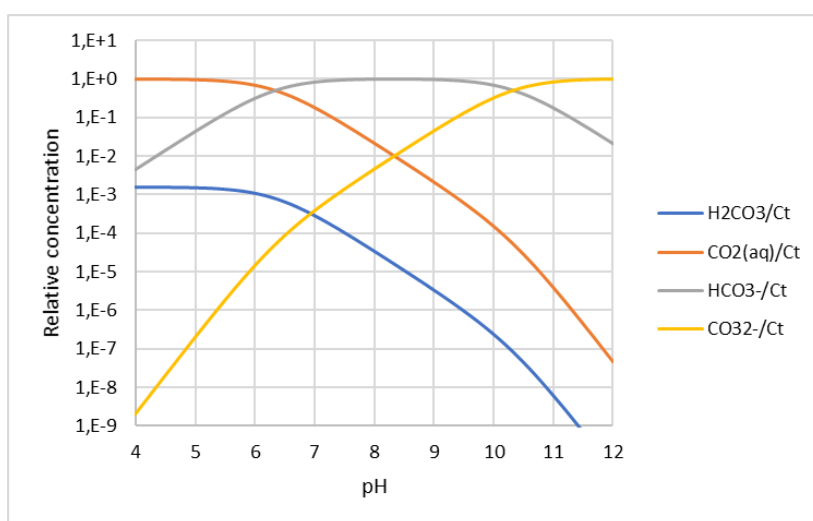
172 When excess calcium hydroxide with pH = 12.65 interact with fresh water with
 173 dissolved CO_2 the equilibria in Eqs. 9-11 will rapidly be displaced to the right and
 174 calcium carbonate will precipitate in an amount corresponding to the *amount of*
 175 *dissolved CO_2 regardless of species:*

176 $\text{Ca}(\text{OH})_2 + \text{CO}_2 (\text{aq}) = \text{CaCO}_3 (\text{s}) + \text{H}_2\text{O}$ (14)

177 If the amount of calcium hydroxide is far above saturation the pH will be unchanged at
 178 the same time as calcium carbonate is precipitating since the solubility of calcium
 179 carbonate is very small (≈ 0.014 g/l). The calcium concentration for saturated calcium
 180 hydroxide is about 22 mM $[\text{Ca}^{2+}]$ and much higher than for saturated calcium carbonate
 181 having 0.14 mM $[\text{Ca}^{2+}]$, a difference of about 150 times. This means that for thinning of
 182 an exactly saturated calcium hydroxide solution, the pH is controlled by dissolved CO_2 :

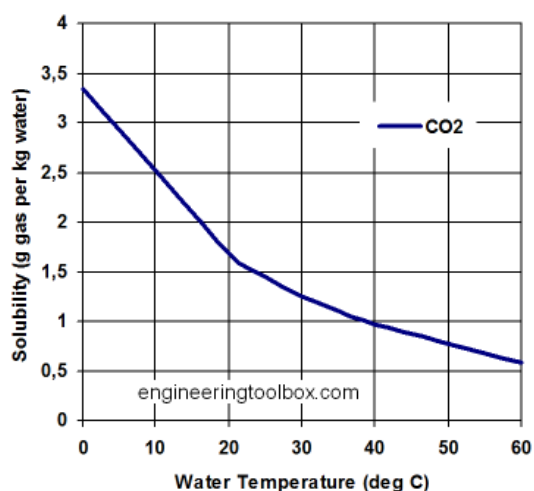
183 $\text{pH} = 14.00 + \log \{2 \cdot ([\text{Ca}(\text{OH})_2] - [\text{CO}_2])\}$ (15)

184



185

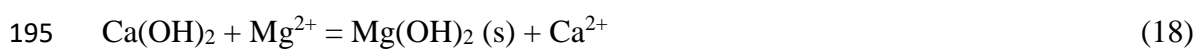
186 **Figure 3** – Distribution of solute species versus pH for a closed aqueous carbonate
 187 system at 25 °C and zero ionic strength [11].



188

189 **Figure 4** – Dissolved CO₂ versus temperature (°C) for carbon dioxide pressure P (CO₂)
 190 = 1 atm [12].

191 In natural fresh water with dissolved alkali carbonate (CO₃²⁻), -hydrogen carbonate
 192 (HCO₃⁻) and magnesium (Mg²⁺) dissolved calcium hydroxide will react as follows:



196 The reactions in Eqs. 16-18 leads to precipitates, since the solubilities at 25°C for calcite,
 197 CaCO₃, is 0.014 g/l or 0.14 mM, and for brucite, Mg(OH)₂, 0.009 g/l or 0.15 mM. Calcite
 198 and brucite are considerably less soluble than portlandite (mineral name for calcium
 199 hydroxide), Ca(OH)₂, with 1.63 g/l or 22mM (a factor of about 150 in molarity).

200 For fresh water saturated with respect to calcium hydroxide, the reactions in Eqs. 16 and
 201 17 will lead to a pH increase since soluble alkali hydroxides will form if the water
 202 contains alkali carbonates or hydrogen carbonates. The reaction in Eq. 18 will lead to a
 203 weak reduction in pH since it will increase the concentration of calcium ions that in turn
 204 will suppress the solubility of calcium hydroxide due to the common ion effect according
 205 to Eq. 4.

206 For fresh water undersaturated with respect to calcium hydroxide, reaction 16 will reduce
 207 pH, reaction 17 not lead to any change and reaction 18 reduce pH if brucite is precipitated.

208 On long term, all calcium hydroxide in fresh water will be converted to calcium carbonate
 209 as there is an unlimited supply of CO₂ relative to calcium hydroxide while the rate is
 210 dependent on the concentration of CO₂. Pure fresh water without dissolved CO₂ in
 211 equilibrium with calcite (CaCO₃) has pH 9.91 [13] but will be somewhat lower if there is
 212 dissolved CO₂ present as well. Based on the calcite solubility of 0.14 mM at 25°C the pH
 213 should be about 10, but there is some uncertainty in the solubility.

214

215

216 1.3 Chemistry of burnt lime (CaO) in sea water

217 Atlantic sea water has typical composition listed in Table 2 and the sum of components
 218 gives a mass of 3.513 %, which is a typical salinity. The sum of positive charge is 0.623
 219 M, while the sum of negative charge is 0.622 M, confirming electroneutrality and that all
 220 major ions are accounted for. Since sea water consists of a mixture of dissolved salts, one
 221 cation does not belong to a specific anion to make a compound.

222 The greatest difference between sea water and fresh water is the content of Na⁺ and Cl⁻.
 223 Sodium chloride is not expected to form compounds with calcium hydroxide, but
 224 according to Duschesne and Reardon [14] the solubility of Ca(OH)₂ increases with
 225 increasing concentration of NaCl due to ion pair formations in their calculations verified
 226 experimentally by Johnston and Grove [15] and by Yeatts and Marshall [16]. If a
 227 simplified version of sea water is 0.5 M NaCl, the solubility of Ca(OH)₂ will increase
 228 from 22 to 28 mM. On the other hand, a number of other ions in sea water will interact
 229 with Ca(OH)₂ and disturb this picture.

230 The second biggest difference is the content of sulphate and much higher concentration
 231 of magnesium. The magnesium will react as described in Eq. 18, while the sulphate ions
 232 will form gypsum:



234 The magnesium reaction (Eq. 18) release calcium ions that suppress hydroxide
 235 concentration and gypsum formation (Eq. 19) will release hydroxyl ions that potentially
 236 reduce the calcium concentration locally relative to solid calcium hydroxide (Eq. 4), so
 237 the overall outcome is complex depending on concentration. According to Table 2 the
 238 molarity of magnesium is 0.0549 M in Atlantic sea water as compared to 0.0289 M for
 239 sulphate, so in sea water the magnesium reaction will dominate.

240

241 **Table 2** – typical composition of Atlantic sea water

Species	M _w (g/mol)	Mass (%)	M (mol/l)
Na ⁺	22.990	1.08	0.4825
Cl ⁻	35.453	1.94	0.5620
Mg ²⁺	24.305	0.13	0.0549
SO ₄ ²⁻	96.063	0.27	0.0289
Ca ²⁺	40.078	0.04	0.0103
K ⁺	39.098	0.04	0.0105
Br ⁻	79.904	0.0067	0.0009
HCO ₃ ⁻	61.017	0.005	0.0008
CO ₃ ²⁻	60.009	0.001	0.0002

242

243 The potential compounds formed by interaction of calcium hydroxide and sea water are
 244 listed in Table 3. The magnesium compounds with higher molar solubility than brucite,

245 Mg(OH)₂, are not expected to form on its expense. An experimental program was then
 246 initiated to measure which compounds that are actually formed when burnt lime is added
 247 to sea water.

248 **Table 3** – Potential compounds that can form by interaction of CaO with sea water

Compounds	M _w (g/mol)	Solubility (g/l)	solubility (mM)
Ca(OH) ₂	74.09	1.77	23.89
CaCO ₃ ^a	100.09	0.014	0.14
Mg(OH) ₂	58.32	0.009	0.15
MgCO ₃ ^b	84.31	0.106	1.26
CaSO ₄ ·2H ₂ O	172.17	2.5	14.52
MgCO ₃ ·Mg(OH) ₂ ·3H ₂ O ^c	196.68	-	-
3MgCO ₃ ·Mg(OH) ₂ ·3H ₂ O ^b	365.31	0.4	1.09
MgCO ₃ ·5H ₂ O ^b	174.39	1.8	10.32
MgCO ₃ ·3H ₂ O ^b	138.36	1.6	11.56

249 ^a Can be found as the polymorphs calcite, aragonite and vaterite which can be
 250 differentiated by XRD.

251 ^b Not expected to form as the molar solubility is greater than for Mg(OH)₂.

252 ^c Solubility not known, but the molar solubility is expected to be greater than for Mg(OH)₂
 253 and it is not likely to form.

254

255 2 MATERIALS AND METHODS

256 2.1 Materials

257 The burnt lime (CaO) used in all tests is of industrial grade from Miljøkalk AS, Norway.
 258 There are two types denoted “Fine, burnt lime” and “Coarse, burnt lime” and the physical
 259 difference can be observed directly in Fig. 5, while the sieving curves are shown in Fig.
 260 6. The sieving was performed in accordance with EN 933-1. Other properties of the burnt
 261 lime samples are given in Table 4.

262

263 **Table 4** – Properties of fine and coarse burnt lime

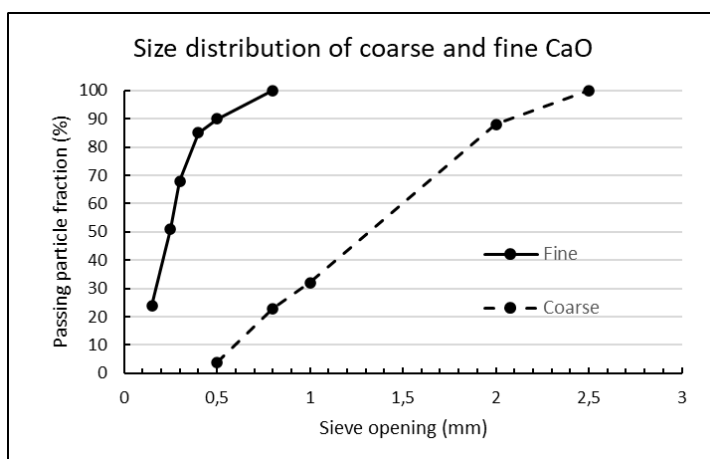
Property	Method	Fine CaO	Coarse CaO
Specific surface (m ² /g)	BET	1.53	1.12
Active CaO (%)	ASTM C25-11 E1	94	91
CO ₂ residue (%)	ASTM C25-11	1.6	2.7
Reactivity in fresh water	EN 459-2		
Time to reach 60°C (sec)		100	250
Semi-adiabatic ΔT (°C)		75	75
Reactivity in sea water	EN 459-2		
Time to reach 60°C (sec)		300	500
Semi-adiabatic ΔT (°C)		70	70



264

265 **Figure 5** – Physical appearance of fine CaO to the left and coarse CaO to the right.

266



267

268 **Figure 6** – Sieving curves for fine and coarse CaO (burnt lime)269 **2.2 Equipment**270 **2.2.1 Characterization tools for the solid phase**

271 *Isothermal calorimetry* of cement pastes was performed with a TAM Air instrument set
 272 to 15°C in closed glass vials. The glass vials were coupled to an external mixing device
 273 with 4 syringes with 1 ml capacity each for injection of either fresh or sea water. 70 mg
 274 of coarse or fine fraction of CaO was weighed into the glass vial, the syringes filled with
 275 4 ml fresh or sea water and the whole arrangement closed in the isothermal calorimeter
 276 for thermal equilibration verified by zero heat flow. The stirring motor was the only part
 277 outside the calorimeter. Each experiment was repeated 3 times and the heat flow curves
 278 used was an average of 3. A dosage of 70 mg CaO/4 ml corresponds to 17.5 g/l.

279 *Thermogravimetric analysis (TGA)* was performed with a Mettler Toledo TGA/SDTA
 280 851. Samples were analysed with a heating rate of 10 °C/min between 40 – 900°C. All
 281 measurements were performed in nitrogen atmosphere with a flow rate of 50 ml/min. The
 282 calcium hydroxide content in a hydrated CaO sample was calculated from the mass loss
 283 between \approx 400-550°C caused by its dehydration. The corresponding temperature range
 284 for thermal dehydration of magnesium hydroxide is 300-400°C and the decarbonation of
 285 precipitated calcium carbonate for temperatures > 600°C. The exact boundaries were
 286 chosen from the peak in the DTG curve.

287 The mineralogy was detected using a Bruker D8-Advance with a generator of x-ray
288 KRISTALLOFLEX K 760-80F (power: 3000W, voltage: 20-60KV and current: 5-80mA)
289 with a tube of RX with copper anode was employed to record the diffractograms of the
290 CaO in the kinetic experiments. All the measurements were taken at 25 °C from 10 to 70
291 2θ with a step size of 0.05° 2θ and 3s time per step.

292 The morphology and the local chemical composition of the materials was explored in the
293 time-course experiments using by Scanning Electron Microscopy (SEM) coupled to
294 Energy Dispersive X-Ray Analysis (EDX). For these analyses a Hitachi S-3000 N
295 Electron Microscope coupled to an EDX Bruker Esprit 1.8 unit was employed.

296 **2.2.2 Analysis in the liquid phase**

297 Fine CaO was added to natural sea water sampled from the Trondheim Fjord, Norway, at
298 temperatures 5 or 15°C in a surplus dosage of 10 g CaO/l during stirring. The experiments
299 were performed in a container open to the atmosphere and the temperature of the
300 surrounding environment was kept constant either by immersion in an ice-water bath (5
301 °C) or kept in a thermostatic room set at 15°C. Before starting the experiments, the water
302 was pre-adjusted to the required temperature by a thermostat.

303 The ion composition of the applied sea water is listed in Table 5. Samples of ≈ 400 μl was
304 drawn from this suspension by a syringe at the times 0 (sea water before addition of CaO),
305 1, 3, 10, 15 and 30 min. The sampled suspension was filtered through 0.45 μm syringe-
306 filter and 100 μl of the filtrate was diluted to 10 ml using MilliQ water and analyzed by
307 Ion Chromatography (Dionex®) for F⁻, Cl⁻, SO₄²⁻, CO₃²⁻ (given as μS/min by the
308 instrument), Na⁺, Mg²⁺, K⁺ and Ca²⁺. The analytical system was based on a double
309 channel so both cations and anions were analyzed under the same run. A Dionex IonPac
310 CS16 column was used for detection of cations while a column Dionex AS18 coupled
311 with a column CG5A was used for measurement of anions. The pH was measured by a
312 pH-meter in a GLP/GMP environment calibrated just before the experiments towards pH
313 = 7.00 and a 10.012 standard, as well as corrected with respect to temperature.

314 **2.2.3 Exposure assays of CaO**

315 Fine CaO was dispersed into sea water in a dosage of 5 g CaO per 500 ml sea water at
316 5°C under slow stirring, and the suspension was kept under constant stirring between each
317 sampling. Solids from the suspensions was rapid filtered off using filter paper on Büchner
318 funnel attached to a vacuum pump followed by washing with 99% ethanol to halt the
319 reaction. The solids were then added to a plastic tube with screw cap together with 15 ml
320 ethanol and shaken for 30 sec. This was followed by centrifugation at 1500 rpm and the
321 liquid phase removed. Finally, the samples were freeze dried under vacuum for 24 h
322 before sealed storage prior to further solid-phase analysis. The sampling was performed
323 after 1, 5, 15 and 30 minutes, as well as after 1, 2, 5, 8, 24 hours (1 day) and 2, 3, 4, 5, 6
324 and 7 days.

325 The solids produced in the time-course transformation experiments were investigated by
326 SEM/EDX for topology and semi-quantitative local chemical composition. X-ray
327 diffraction (XRD) was applied to follow qualitatively how the crystalline phases
328 developed as a function of time, while TGA was used to determine the content of some
329 phases quantitatively.

330

331 **3 RESULTS**332 **3.1 Influence of burnt lime on sea water composition as function of time**

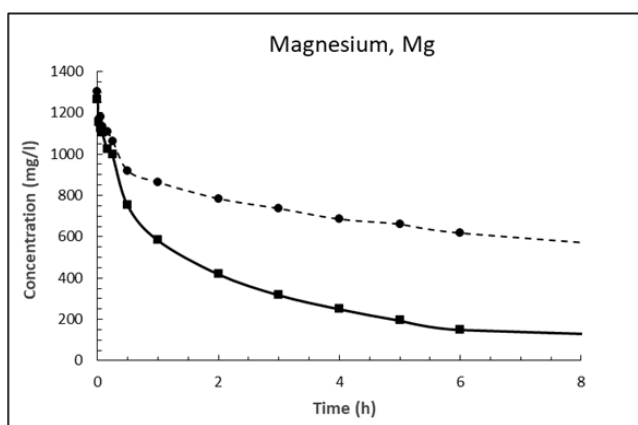
333 The salinity of the applied sea water in Table 5 is 3.448%, which is marginally lower than
 334 average Atlantic sea water given in Table 2 (3.513%). The sum of positive charge is
 335 0.6149 mol/l while the sum of negative charge is 0.5824 mol/l. The lack of negative
 336 charge ($\Delta = 0.0325$ mol/l) is attributed to lack of carbonate and hydrogen carbonate.

337 **Table 5** – Major ion composition and pH of the sea water used

Species	M_w (g/mol)	ppm	M (mol/l)
Na^+	22.990	10981.1	0.4776
Cl^-	35.453	18553.6	0.5233
Mg^{2+}	24.305	1301.6	0.0536
SO_4^{2-}	96.063	2835.3	0.0295
Ca^{2+}	40.078	399.0	0.0100
K^+	39.098	394.0	0.0101
Br^-	79.904	0.05	0.0000
F^-	18.998	1.25	0.0001
pH	-	7.88	-

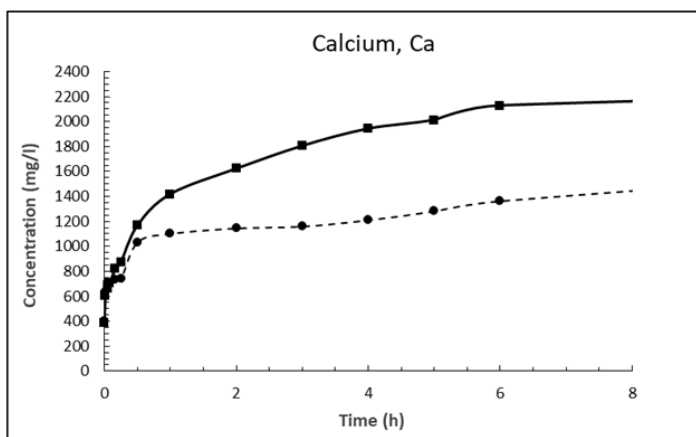
338

339 The dosage of 10 g/L CaO in sea water corresponds to 13.2 g/L $\text{Ca}(\text{OH})_2$, which is about
 340 8 times higher than its solubility. The result is a white suspension often referred to as
 341 «milk of lime». The evolution of magnesium (Mg^{2+}), calcium (Ca^{2+}), sulphate (SO_4^{2-}),
 342 carbonate (CO_3^{2-}) and pH in sea water as a function of time until 8 h after addition of
 343 burnt lime are plotted in Figs. 7, 8, 9, 10 and 11, respectively. The ion concentrations after
 344 24 h are presented in Table 6.



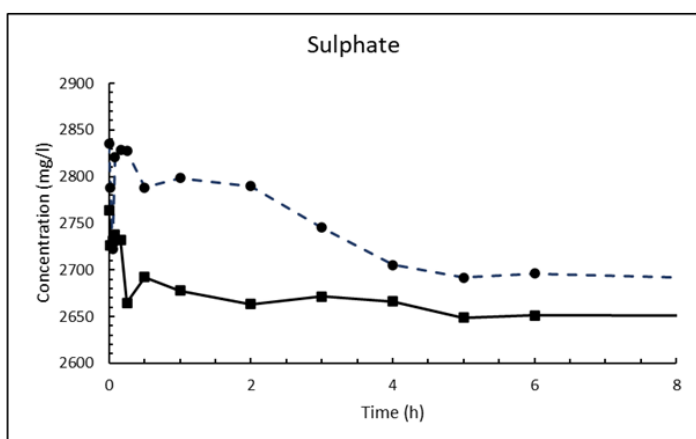
345

346 **Figure 7** – Concentration of magnesium in sea water at $T = 5^\circ\text{C}$ (dashed line) and 15°C
 347 (solid line) as function of time after adding 1% (w/V) fine CaO.



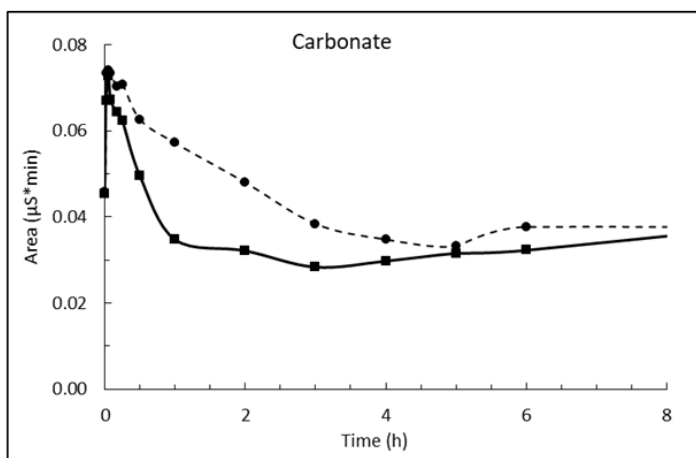
348

349 **Figure 8** – Concentration of calcium in sea water at $T = 5^{\circ}\text{C}$ (dashed line) and 15°C (solid
 350 line) as function of time after adding 1% (w/V) fine CaO.



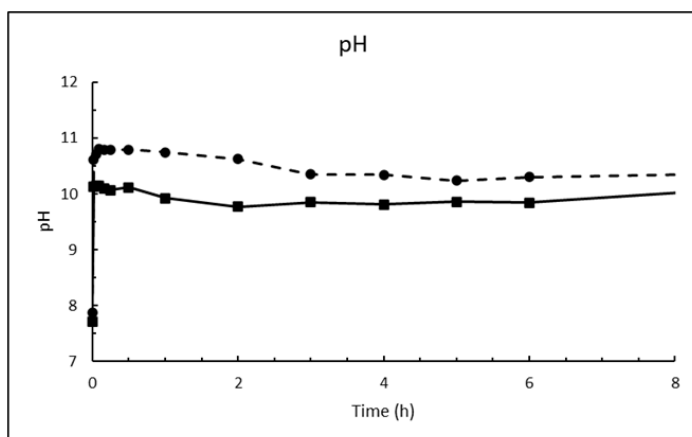
351

352 **Figure 9** – Concentration of sulphate in sea water at $T = 5^{\circ}\text{C}$ (dashed line) and 15°C
 353 (solid line) as function of time after adding 1% (w/V) fine CaO.



354

355 **Figure 10** – Relative concentration of carbonate in sea water at $T = 5^{\circ}\text{C}$ (dashed line) and
 356 15°C (solid line) as function of time after adding 1% (w/V) fine CaO.



357

358 **Figure 11** – pH in sea water at $T = 5^{\circ}\text{C}$ (dashed line) and 15°C (solid line) as function of
 359 time after adding 1% (w/V) fine CaO.

360

361 **Table 6** – Compositional change of sea water at 5 and 15°C the first 24 h after adding
 362 1% w/V fine CaO

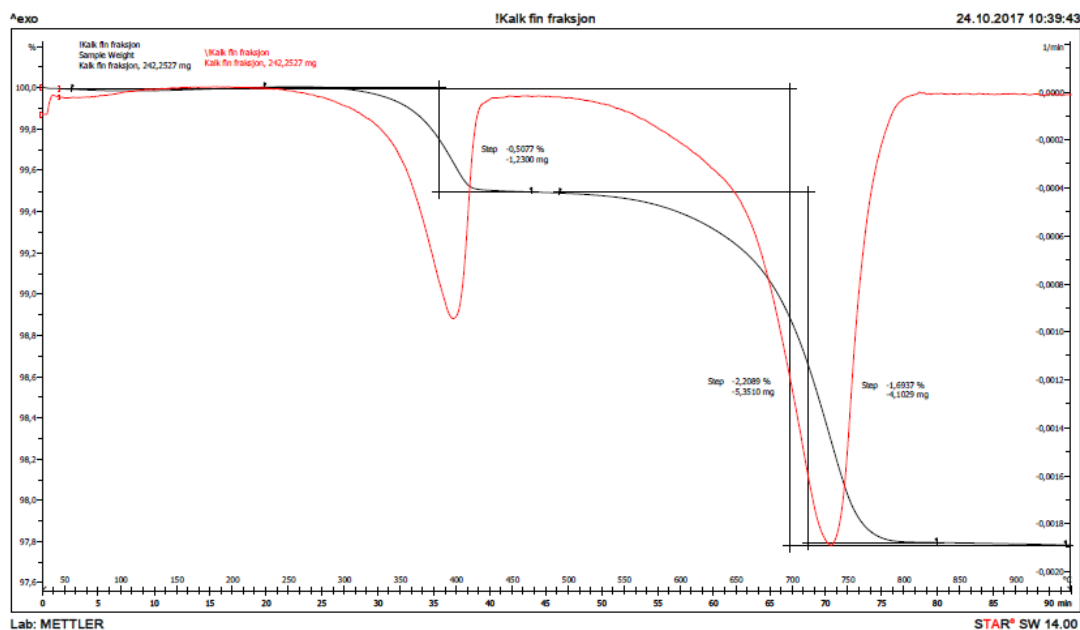
Species	Temperature 5°C		Temperature 15°C	
	Time 0 h	Time 24 h	Time 0 h	Time 24 h
Magnesium, Mg^{2+}	1302 mg/l	236 mg/l	1265 mg/l	2.1 mg/l
Calcium, Ca^{2+}	399 mg/l	2056 mg/l	386 mg/l	2361 mg/l
Sulphate, SO_4^{2-}	2835 mg/l	2662 mg/l	2764 mg/l	2648 mg/l
Carbonate, CO_3^{2-}	$0.046 \mu\text{S}\cdot\text{min}$	$0.035 \mu\text{S}\cdot\text{min}$	$0.045 \mu\text{S}\cdot\text{min}$	$0.061 \mu\text{S}\cdot\text{min}$

363

364 **3.2 Change of solids composition as function of time for CaO in contact with sea** 365 **water**

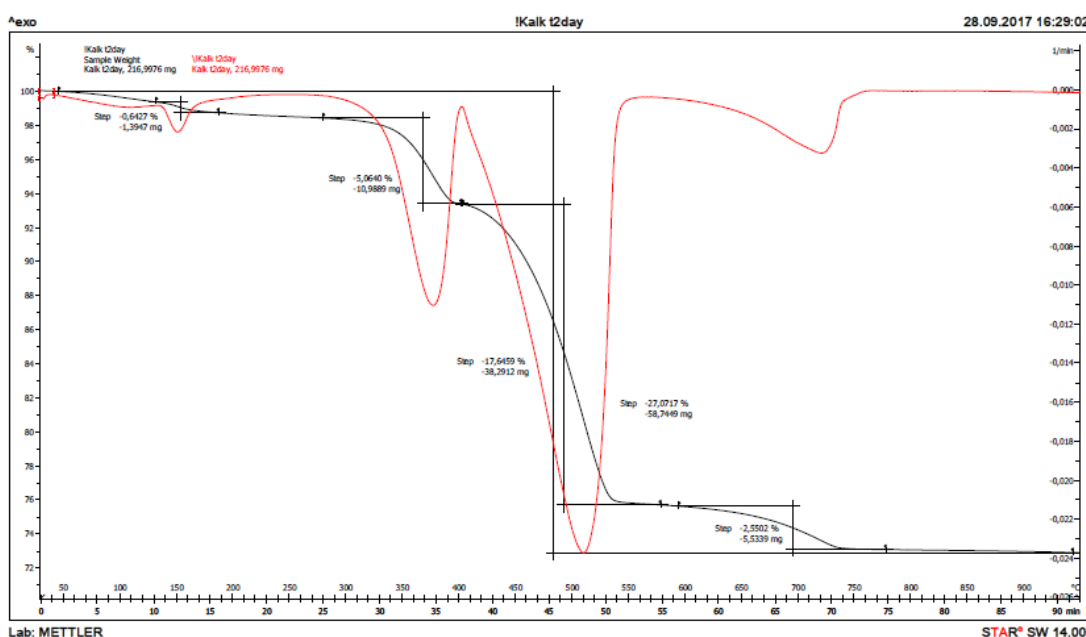
366 The result from thermogravimetry, TG (mass loss as function of temperature) is plotted
 367 in Fig. 12 for fine, burnt lime (CaO) as received and in Fig. 13 for the solids obtained
 368 after 1% CaO has been dispersed in sea water for 2 days. The signal with maximum for
 369 the derived curve (DTG) at $\approx 400^{\circ}\text{C}$ in Fig. 12 figure is due to the decomposition of
 370 $\text{Ca}(\text{OH})_2$ to CaO and H_2O , while the signal at $\approx 740^{\circ}\text{C}$ is caused by decomposition of
 371 CaCO_3 to CaO and CO_2 . The signal just looks large in this accurate measurement due to
 372 the scale, but the bulk calculation from the curves only calculates to 2.09% $\text{Ca}(\text{OH})_2$ and
 373 3.85% CaCO_3 with the remainder being 94.06% CaO. The XRD of the same sample
 374 revealed largely signals from CaO with traces of $\text{Ca}(\text{OH})_2$ and CaCO_3 . It is difficult to
 375 avoid that a material as reactive as fine CaO will pick up some moisture and maybe carbon
 376 dioxide from air during handling.

377



378

379 **Figure 12** – The thermogravimetry curves (TG) in black and its derivative (DTG) in red
 380 for fine CaO as received.



381

382 **Figure 13** – The thermogravimetry curves (TG) in black and its derivative (DTG) in red
 383 for the solids of 1% CaO dispersed in sea water for 2 days.

384 Similar calculations as for received CaO can be done when it has been reacting with sea
 385 water for some time, for instance from the curves after 2 days reaction in Fig. 13. The
 386 signals with maxima at ≈ 140 , 370, 510 and 730°C are due to thermal decomposition of
 387 gypsum (looses 2 water molecules), magnesium hydroxide (looses 1 water molecule),
 388 calcium hydroxide (looses 1 water molecule) and calcium carbonate (looses 1 molecule
 389 carbon dioxide). From the TG/DTG data, the bulk composition of solids from reaction of
 390 CaO with sea water in any point in time can be calculated for the 5 phases: $\text{CaSO}_4 \cdot \text{H}_2\text{O}$
 391 (gypsum), $\text{Mg}(\text{OH})_2$ (brucite), $\text{Ca}(\text{OH})_2$ (portlandite), CaCO_3 (sum of crystal

392 modifications calcite, aragonite and vaterite), as well as remaining CaO (burnt lime) from
 393 the material mass weighed in, after subtracting the other 5 phases. The chemical reasoning
 394 in section 1.3 postulate that only these phases will be present, and this is also confirmed
 395 by XRD after reacting 1% CaO with sea water for 2 days. The bulk composition of solids
 396 as a function of reaction time for 1% fine CaO in sea water is shown in Table 7 for the
 397 first day and in Table 8 for a week, while the content of remaining CaO is plotted in Fig.
 398 14. The deviation from 100% in Tables 7 and 8 is due to adsorbed moisture. The results
 399 reveal that more than 97% CaO has reacted after 1 day and as much as 96% after just 5
 400 hours.

401 **Table 7** – Bulk composition of solids from reaction of 1% fine CaO with sea water
 402 versus time at 5°C for the first 24 h.

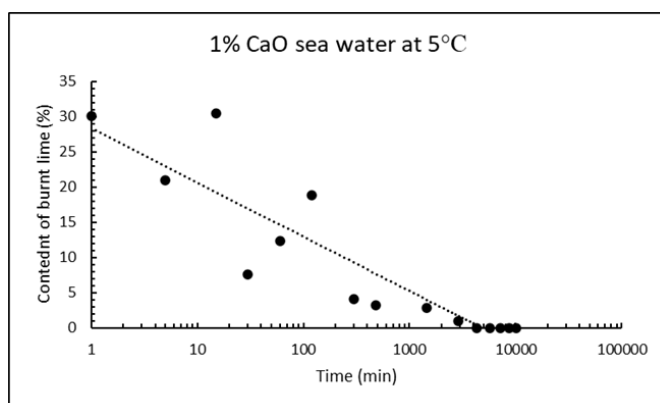
Time	1 min	5 min	15 min	30 min	1 h	2 h	5 h	8 h	24 h
Time (min)	1	5	15	30	60	120	300	480	1440
Gypsum	0.0	0.0	0.0	0.0	0.7	0.0	8.5	4.3	0.4
Mg(OH) ₂	9.0	17.7	7.1	14.8	16.1	5.0	17.0	15.2	12.7
Ca(OH) ₂	50.4	49.0	55.4	66.2	61.3	70.3	62.7	69.9	76.4
CaCO ₃	7.7	8.2	5.7	8.7	7.0	4.9	6.4	6.0	6.3
CaO	30.1	20.9	30.4	7.6	12.3	18.8	4.2	3.2	2.9
Sum	97.3	95.8	98.6	97.3	97.5	99.0	98.8	98.6	98.7

403

404 **Table 8** – Bulk composition of solids from reaction of 1% fine CaO with sea water
 405 versus time at 5°C for 1-7 days.

Time	1 d	2 d	3 d	4 d	5 d	6 d	7 d
Gypsum	0.4	3.1	8.4	5.3	5.8	9.5	8.2
Mg(OH) ₂	12.7	16.4	17.6	12.3	21.3	16.0	14.7
Ca(OH) ₂	76.4	72.6	64.6	73.4	62.2	68.8	70.0
CaCO ₃	6.3	5.8	8.6	8.5	9.7	5.3	6.4
CaO	2.9	1.0	0.0	0.0	0.0	0.0	0.0
Sum	98.7	98.8	99.2	99.4	99.0	99.6	99.3

406

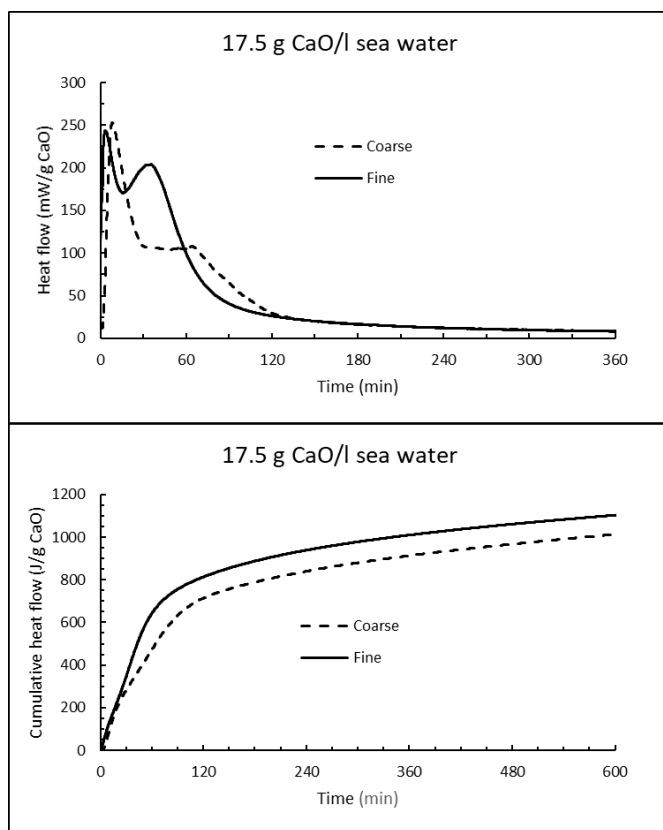


407

408 **Figure 14** – Remaining content of CaO as a function of time after 1% fine CaO have
 409 been mixed in sea water at 5°C.

410 The reactivity of CaO have also been followed by isothermal calorimetry at 15°C. The
 411 average heat flow curves (mW/g CaO) for 3 parallel samples at dosage 17.5 g CaO/l are
 412 compared for fine and coarse burnt lime at the upper part of Fig. 15, while the
 413 corresponding cumulative heat curves are plotted at the lower part of Fig. 15. The heat
 414 flow curves have a bimodal form with a first immediate rapid reaction rate and a
 415 secondary increase in the range 30 min (fine CaO) to 70 min (coarse CaO). The secondary
 416 reaction was more pronounced for fine CaO. Note that a point on the heat flow curve in
 417 Fig. 15 (upper part) represent the *rate* of an exothermal reaction while the slope of an
 418 increasing curve represents *acceleration*. For the cumulative heat in Fig. 15 (lower part),
 419 a value of about 928 J/g CaO corresponds to a reaction degree of $\approx 80\%$ since the reaction
 420 heat for burnt lime in pure water is 1160 J/g CaO, unless there are other exothermal
 421 reactions involved like precipitation of brucite. According to the plots in Fig. 15, coarse
 422 CaO release 928 J/g (80% reaction) after 390 min, while fine CaO develop same amount
 423 of energy in 226 min. Note that the reaction rate under adiabatic conditions (developed
 424 heat is conserved and temperature rises as in Tables 1 and 4) will be much faster than
 425 under isothermal condition (i.e. constant temperature) as in Fig. 15.

426



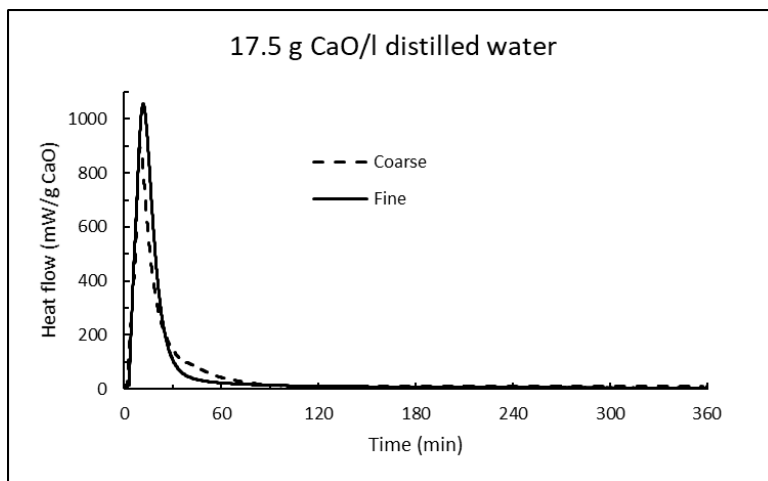
427

428

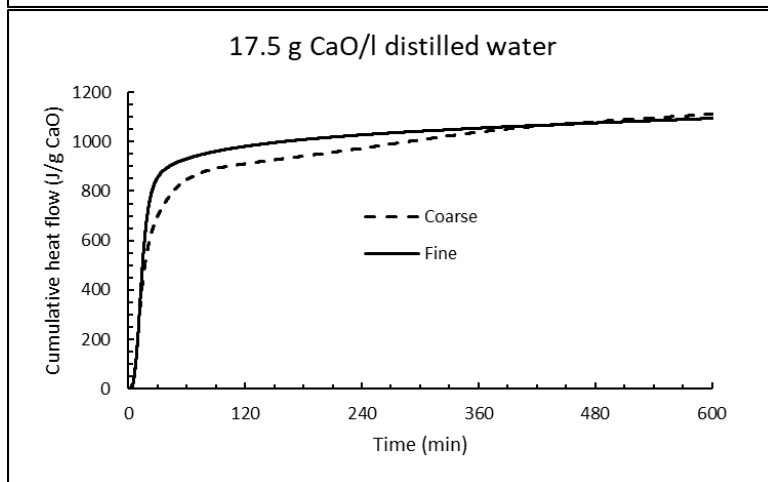
429 **Figure 15** – The heat flow (top) and cumulative heat (bottom) under isothermal
 430 conditions at 15°C when 17.5 g CaO is mixed with 1 litre sea water.

431 Analogous isothermal experiments as for sea water were performed for 1.75 g CaO per
 432 litre distilled water at 15°C. The heat flow curves for fine and coarse CaO are plotted at
 433 the upper part of Fig. 16, while the corresponding cumulative heat curves are shown at
 434 the lower part of Fig. 16. Evidently the reaction of burnt lime in fresh water is much more

435 intense than in sea water. The time for coarse CaO to reach 928 J/g was 154 min (less
 436 than half of that in sea water), while fine CaO used 58 min to reach the same heat
 437 evolution compared to 226 min in sea water.
 438



439



440

441 **Figure 16** – The heat flow (top) and cumulative heat (bottom) under isothermal
 442 conditions at 15°C when 17.5 g CaO is mixed with 1 litre distilled water.

443

444 4 DISCUSSION

445 4.1 Influence of burnt lime on sea water composition as function of time

446 When comparing the evolution of magnesium in Fig. 7 with that of calcium in Fig. 8 one
 447 notice that the concentration of magnesium drops while concentration of calcium
 448 increases correspondingly. This is in accordance with Eq. 18 postulated from a chemical
 449 consideration. From Table 7 it is evident that the concentration of magnesium in sea water
 450 at 15°C has dropped 1263 mg/l after 24 h while the concentration of calcium has increased
 451 by 1975 mg/l. Considering the atomic mass of Mg being 24.305 g/mol and that of Ca
 452 being 40.078 g/mol, this corresponds to a drop of magnesium of 52 mM and an increase
 453 in calcium of 49 mM which is equal in light of measurement uncertainty. The
 454 corresponding numbers at 5°C are a 44 mM drop for magnesium and a 41 mM increase
 455 for calcium, again about equal.

456 The reason why the ion exchange between calcium and magnesium is faster at 15°C than
 457 at 5°C the first 8 h (see Figs. 7 and 8) is that it is likely diffusion controlled and diffusivity
 458 is lower at lower temperatures. The temperature dependence of diffusion coefficients [17]
 459 can be expressed by

$$460 \quad D_{(T)} = D_{(T_{ref})} \cdot \exp \left\{ \frac{\Delta E_a}{R} \left(\frac{1}{T_{ref}} - \frac{1}{T} \right) \right\} \quad (20)$$

461 where

462 ΔE_a = activation energy for the reaction (assumed 40 kJ/Mol)

463 R = universal gas constant = 8.3144598 J/K·mol

464 T_{ref} , e.g. 288.15 K (15°C) versus T = 278.15 K (5°C) in this case.

465

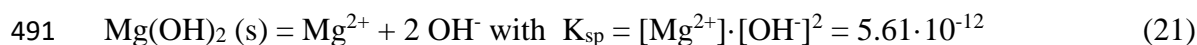
466 The ratio between the diffusion coefficients at 15 and 5°C is 1.8 using the numbers for
 467 Eq. 20. The drop in magnesium concentration after 3 h is 948 and 566 mg/l at 15 and 5°C,
 468 respectively, giving a ratio of 1.67. Using the numbers for calcium gives a corresponding
 469 ratio of 1.86. This is a strong indication that the $\text{Ca}^{2+} \leftrightarrow \text{Mg}^{2+}$ replacement in the material
 470 is diffusion controlled.

471 The change in sulphate concentration is somewhat chaotic to start with as seen from Fig.
 472 9. It is possible that precipitated magnesium hydroxide blocks some of the surface of the
 473 CaO particles in the start, but after a while the concentration decreases successively until
 474 it flattens out until 24 h being the latest measuring point. The solubility of gypsum is 1.82
 475 g/l and 1.96 g/l at 5 and 15 °C, respectively, which corresponds to 1020 and 1090 mg
 476 SO_4^{2-} /l. The measured concentrations are far higher than that (2662 and 2648 mg/l) after
 477 24 h and shows that the reaction between sulphate anions and calcium hydroxide to
 478 gypsum (Eq. 19) is a relatively slow process. The decay in in the sulphate concentration
 479 in the first 24 h is not more than 4-6%.

480 The carbonate concentration drops and levels out on a plateau when 1% fine CaO is added
 481 sea water (Fig. 10). The value of the plateau cannot be compared to the solubility of
 482 calcium carbonate since it is not an absolute value, but a relative value measured as the
 483 area under a curve.

484 The change in pH as function of time when 1% fine CaO is added sea water in Fig. 11
 485 shows that pH increases rapidly (within 1 min) from the pH of sea water of 7.88 at 5°C
 486 and 7.72 at 15°C to 10.61 and 10.13, respectively. The low measured pH relative to
 487 calcium hydroxide is because the CaO dosage was so small that Mg^{2+} was not depleted
 488 as seen from Fig. 7. Hence, the pH is regulated by precipitated magnesium hydroxide.
 489 This will also be the case at open sea where magnesium is in excess.

490 The dissolution of magnesium hydroxide can be written as;



492 Dispersing magnesium hydroxide in fresh water means that $[\text{OH}^-] = 2 [\text{Mg}^{2+}]$ and $[\text{OH}^-]$
 493 $= \sqrt[3]{2K_{sp}} = 2.2 \cdot 10^{-4}$ corresponding to pH = 10.35. From Fig. 7 it can be seen that after 8
 494 h at 15°C $[\text{Mg}^{2+}] = 149 \text{ g/l} = 6.13 \text{ mM}$ and $[\text{OH}^-] = \sqrt{K_{sp}/[\text{Mg}^{2+}]} = 29.8 \cdot 10^{-6}$
 495 corresponding to pH = 9.47 while it is measured 9.84. This is just serving as an illustration
 496 and it is without taking into temperature effect or complex ions etc. At 5°C it seems like
 497 situation is far from equilibrium. At open sea where magnesium is in surplus and
 498 concentration is 53.6 mM (Table 4), the pH at equilibrium would have been reduced to

499 9.01 at 25°C and lower than that at lower temperatures since solubility of magnesium
500 hydroxide decreases with decreasing temperature (0.009 g/l at 18°C and 0.04 g/l at 100°C
501 [18]) unlike calcium hydroxide(Eq. 3).

502

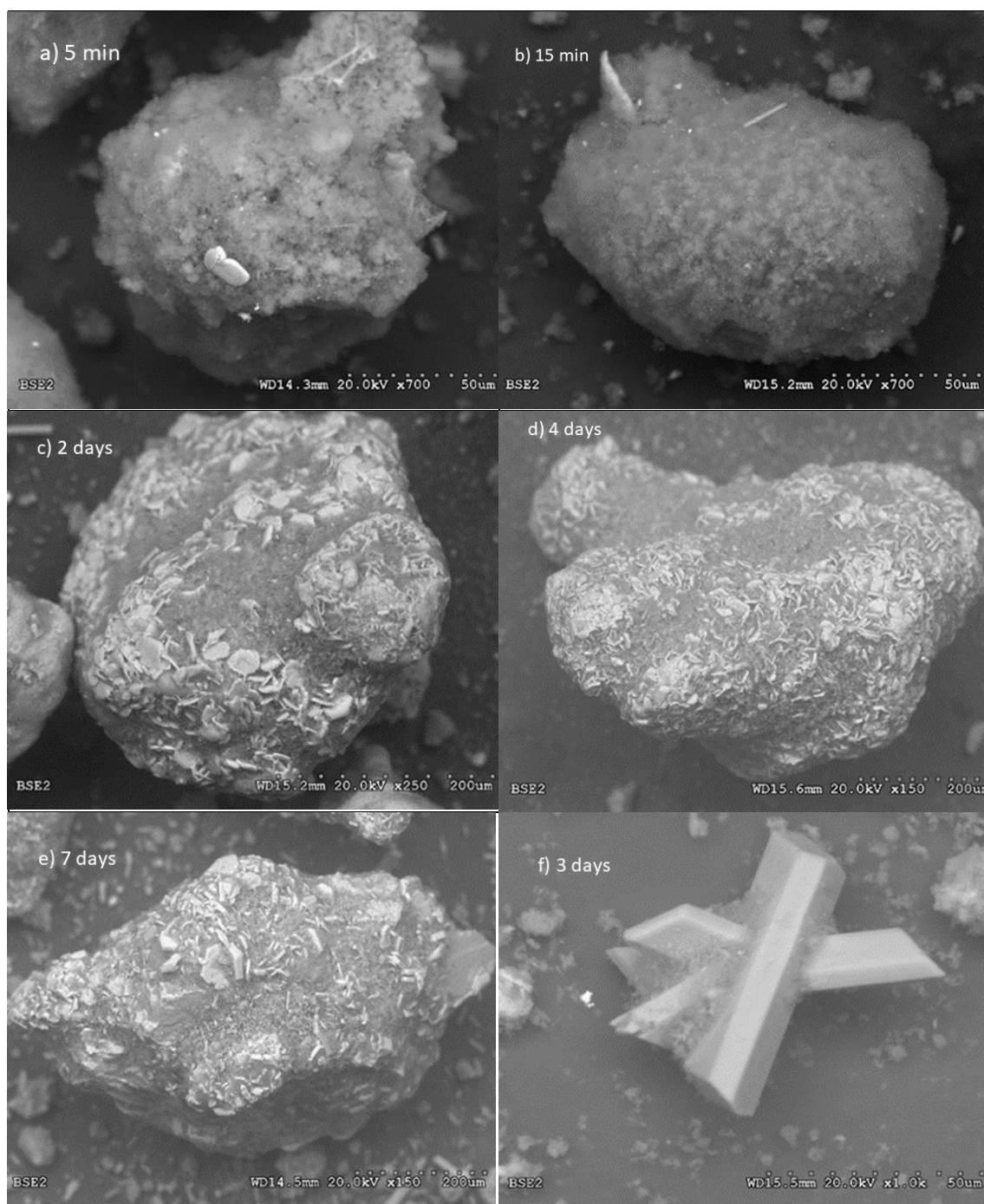
503 **4.2 Change of solids composition as function of time for CaO in contact with sea** 504 **water**

505 The results in Table 7 reveal that calcium hydroxide is formed immediately (first minute)
506 and in a relatively large amount when 1% fine CaO is mixed with sea water at 5°C, since
507 only water is needed, and it is in large excess. Magnesium hydroxide and calcium
508 carbonate are also formed relatively quickly even though the amounts of reactants are
509 limited in this “closed system” and is controlled by amount of CaO relative to sea water
510 and the content of magnesium and carbonate in the sea water. In practical applications
511 the system is “open”, and the supply of reactants are unlimited. The availability of
512 reactants then relies on a combination of current/convection and diffusion of species.

513 It is noticeable from Table 7 that the formation of gypsum occurs slower than the other
514 compounds and appears first after 5 hours. The presence at this time is confirmed by XRD
515 and can be seen as prismatic crystals by SEM in Fig. 17. Another feature disclosed by
516 SEM is that a grey mass is precipitated early on the particle. This is likely to be
517 magnesium hydroxide and may be the reason why burnt lime hydrates slower in sea water
518 than in fresh water as seen from the calorimetry curves in Figs. 15 and 16. Later calcium
519 hydroxides crystallizes to hexagonal plates in line with its crystal structure that penetrates
520 through the precipitated mass of magnesium hydroxide. Examples of this are shown in
521 Fig. 17 and can be compared to the reaction model sketched in Fig. 20 a-f.

522 Images a) and b) in Fig. 17 depicts seemingly amorphous precipitations (likely
523 magnesium hydroxide) on the lime particles after 5 and 15 min, respectively, while image
524 c) after 2 days shows that calcium hydroxide has crystallized to small hexagonal plates
525 penetrating the precipitated grey mass on the particle surface. Magnesium hydroxide will
526 appear darker grey than calcium hydroxide since it is composed of lighter elements, but
527 the physical density may also affect the grey levels. Hexagonal crystals of calcium
528 hydroxide also appears on the particle surface after 4 d in image d) and image e) shows
529 various crystal shapes on the particle surface after 7 days. Image f) focuses on well-
530 crystallized prisms of gypsum at an age of 3 days. Note that the magnification indicated
531 by the dotted line at the bottom of the images is 50 μm for image f) and 200 μm for the
532 other images.

533



534

535 **Figure 17** – A selection of images from the SEM investigation as a function of time.

536

537 4.3 Burnt lime added to sea water in an “open system”

538 Very few trials have been performed to measure pH when burnt lime has been dosed
539 directly to open sea. In such an “open system” will the calcium hydroxide formed during
540 hydration have access to magnesium and other components for neutralization, and pH
541 will be a question of time and distance from individual burnt lime particles.

542 The following test was performed in the river Murray in Canada as described in the
543 DFARD Tech Report #253 [19]: The sea water just outside the river mouth had pH 8.1,
544 while the pH in a trough of slaked lime (i.e. calcium hydroxide) was measured to 12.6.
545 When the slaked lime was thrown into the sea, the pH within the cloud of particles was
546 up to 9. The sea water about 10 m from the trough, but directly above the treatment zone,
547 had pH in the range 8.2-8.3. The pH values dropped rather rapidly back to the natural
548 background level of 8.1 close to the treatment zone.

549 In 2017 [20] and experiment was performed in the Slettnes fjord near Hammerfest in
550 northern Norway, where a suspension of burnt lime was spread over the sea where pH-
551 meters were mounted at 4.98 and 6.28 m depths. A photo of the boat spraying lime
552 suspension is shown in Fig. 18, while the pH logs for the whole period (2 h and 24 min)
553 are plotted in Fig. 19.

554 The measurement at depth 4.98 m starts at 7.77 and climbs to pH 8 within 20 min after
555 spraying starts and the highest pH measured within the period of 2 h and 24 min was 8.08.
556 The measurement at depth 6.28 m started with pH 7.17 and climbed to 7.92 within 20
557 min and stabilized at 7.99 within the measurement period and with 8.04 as the highest
558 value read. It is worth noting that all values measured are within the range to be expected
559 in natural sea water.

560 The measured pH at open sea is in line with the pH estimation < 9 using Eq. 21 and sea
561 water concentration of Mg^{2+} at temperatures $< 20^{\circ}C$.

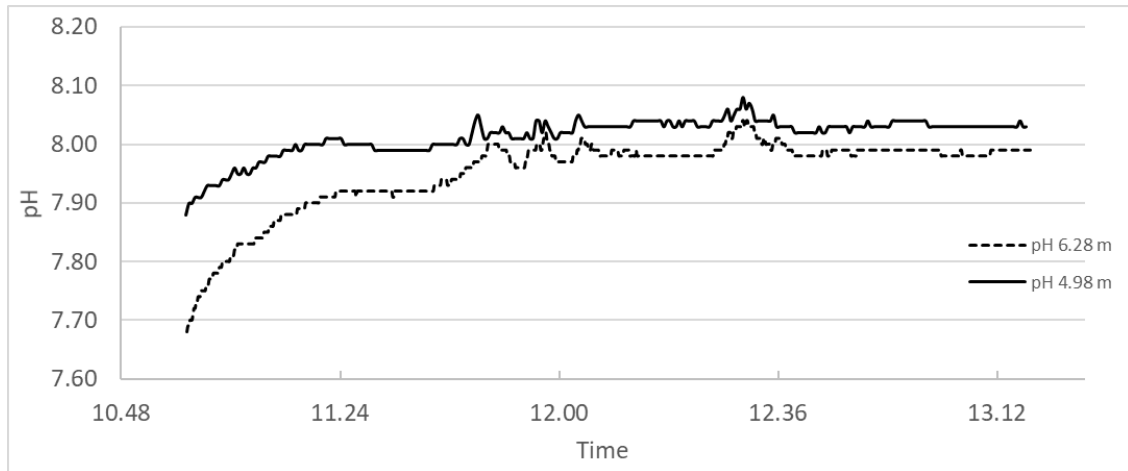
562 Based on the experimental data retrieved and theoretical evaluation, the reaction progress
563 when burnt lime is mixed into the sea can be described as sketched in Figs. 20 a-f.



564

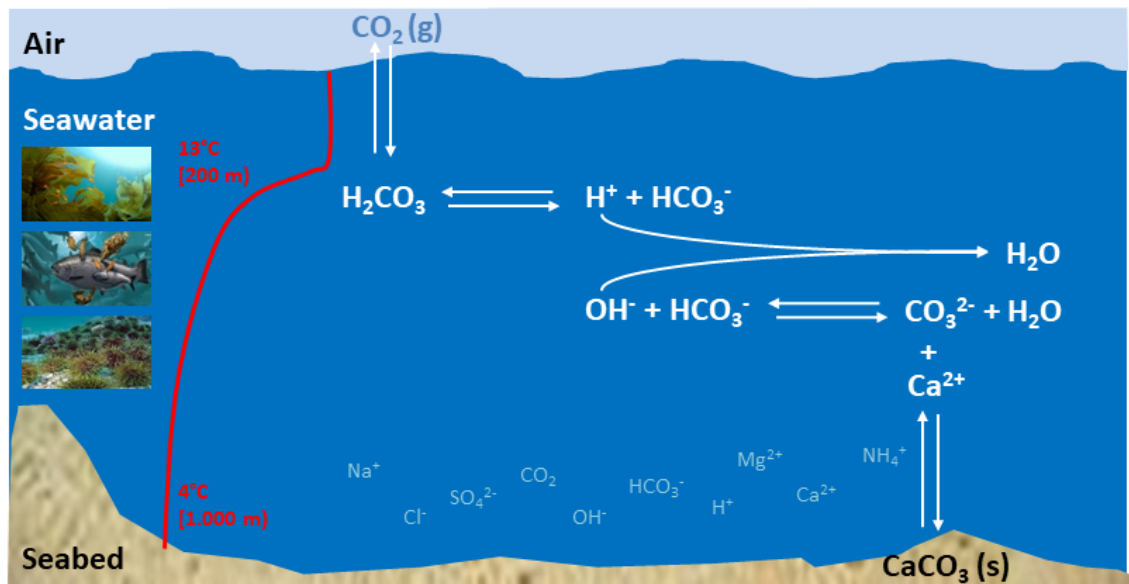
565 **Figure 18** – Photo of the boat spraying lime suspension of coarse CaO over the sea.

566



567

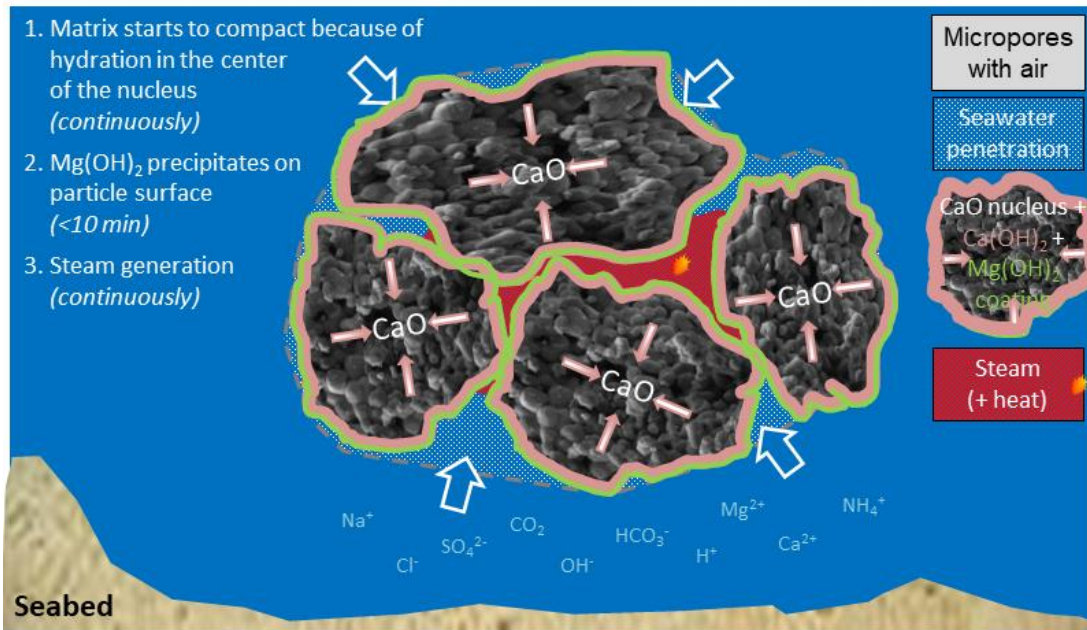
568 **Figure 19** – pH measured in open sea in the area where a suspension of coarse CaO was
 569 sprayed.



570

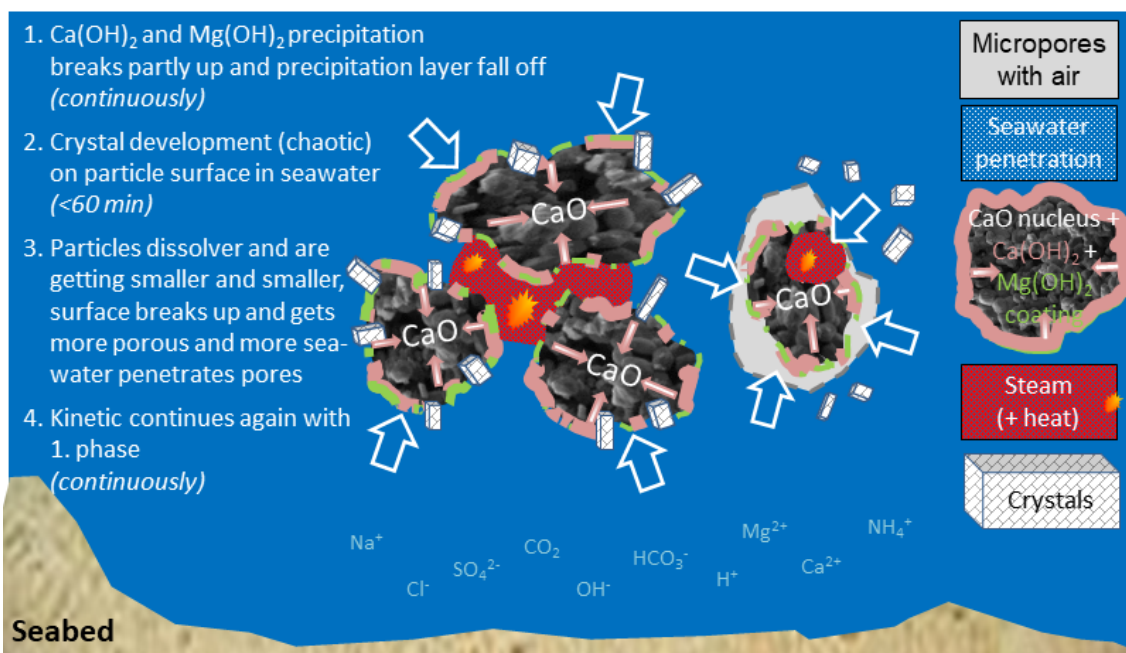
571 **Figure 20a** – Sketch of the «open system» sea water with temperature profile and
 572 different ions.

573



580

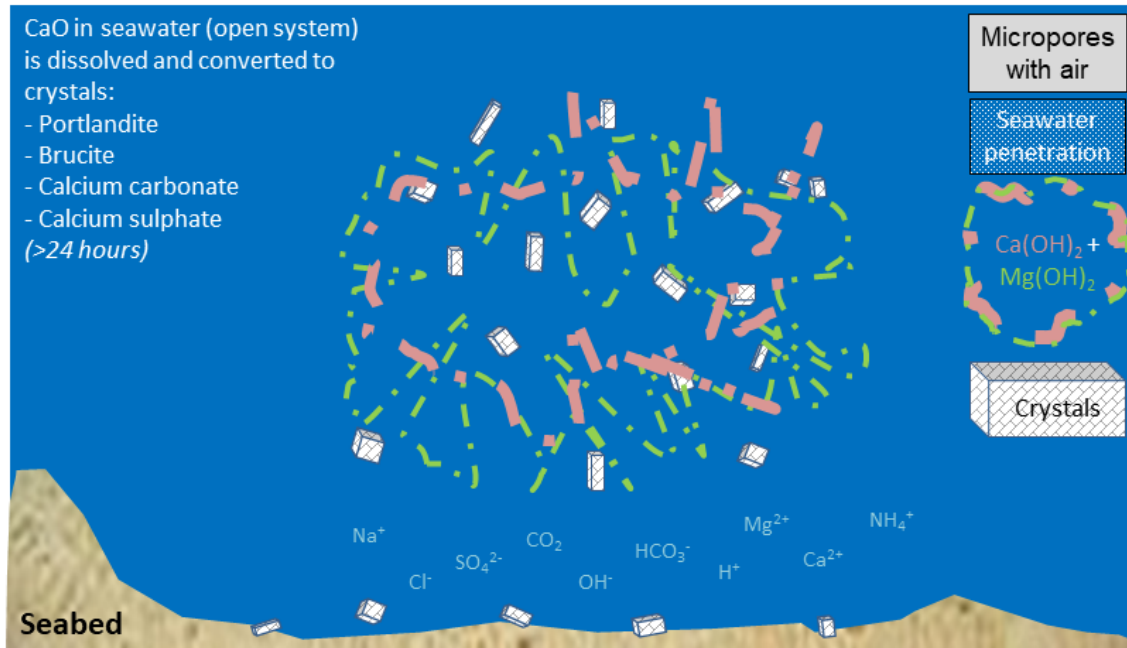
581 **Figure 20d – Phase 2:** The surface reaction forming calcium hydroxide continues and
 582 magnesium hydroxide is precipitated.



583

584 **Figure. 20e – Phase 3:** Structural compression and formation of crystals.

585



586

587 **Figure 20f – Phase 4:** All burnt lime particles are completely reacted and transformed
588 to other solids.

589

590 5 CONCLUSIONS

591 The reaction of burnt lime in sea water has been discussed and compared to fresh water.

592 A particle of burnt lime (CaO) added to sea water will immediately react to form calcium
593 hydroxide (called slaking) and more than 90% of the lime would have reacted within 5
594 hours in a “closed system”. This process is expected to be even faster in an “open system”
595 such as the open sea or a fjord. The slaking process is extremely exothermic and will be
596 able to increase the temperature of the surroundings of the particles. However, a
597 remarkable or persistent increase of local sea water temperature would be extremely
598 unlikely due to the low doses applied and the large water reservoir.

599 The reaction of burnt lime in sea water is slower than in fresh water. This is, probably due
600 to the large concentration of magnesium in sea water, that provokes a rapid precipitation
601 of magnesium hydroxide onto the surface of the particle and hinders the progress of the
602 hydration reaction of CaO.

603 The slaking process will increase pH locally from the natural level of about 8 to a
604 theoretical maximum of 12.5 near the surface of the particle on a micro level. In an “open
605 system” the pH will be within the variation in natural sea water (7.8-8.5) a few cm away
606 from the particle, as shown in practical field experiments.

607 In parallel to the slaking process, dissolved calcium hydroxide will react with magnesium
608 ions in sea water and precipitate less soluble magnesium hydroxide. The equilibrium pH
609 of magnesium hydroxide in fresh water is 10.5, but in equilibrium with the magnesium
610 concentration in seawater it is calculated to < 9 as observed.

611 All carbonate, hydrogen carbonate and dissolved CO₂ in the vicinity of formed calcium
612 hydroxide will be consumed and yield calcium carbonate. Same happens with sulphate,
613 that will react and form gypsum, but somewhat slower than the magnesium and carbonate
614 reactions. It is likely however that the magnesium reaction will dominate in an “open
615 system”.

616 The product formed at equilibrium after dosing burnt lime in the sea will be a mixture of
617 magnesium hydroxide (that possibly will be slowly converted to magnesium carbonate
618 over time), calcium carbonate and gypsum (i.e. calcium sulphate dihydrate). All calcium
619 oxide and hydroxide will be consumed and no traces of them will remain at equilibrium.
620 How long time that will take depends on the thinning rate probably being a function of
621 the particle size, the temperature and the water renewal due to natural currents.
622 Correspondingly will all dissolved calcium be diluted and eventually reach the natural
623 background level of sea water. According to the data retrieved in this study, the reaction
624 will be complete within a few days or maximum a week. It is worth noting that all of the
625 final products magnesium carbonate, calcium carbonate and gypsum all occur naturally
626 and can be regarded harmless for the environment.

627

628 **Acknowledgements**

629 This work was supported by grants 217663 and 269272 from the Research Council of
630 Norway. Flagship Fjord and Coast at the Fram Centre in Tromsø helped to facilitate the
631 field work. Thanks to Alf Børre Tangeraas who assisted during the lab and field trials, to
632 Franzefoss AS for financial and practical support, and to Cermaq ASA for help with
633 logistics and all the other support we have asked for.

634

635 **References**

- 636 [1] Brooks, S.J., Georgantzopoulou, A., Johansen, J.T., Mengede, M. “Determining the
637 risk of calcium oxide (CaO) particle exposure to marine organisms”, *Marine*
638 *Environmental Research* (2020), doi: <https://doi.org/10.1016/j.marenvres.2020.104917>
639 [2] Strand, H.K., Christie, H., With Fagerli, C., Mengede, M. and Moy, F. “Optimizing
640 the use of quicklime (CaO) for sea urchin management — a lab and field study”,
641 *Ecological Engineering: X* (2020), doi: <https://doi.org/10.1016/j.ecoena.2020.100018>
642 [3] J. Wuhler: "Physikalisch-chemische Untersuchungen über den Zustand des
643 Branntkalkes und über die Vorgänge und Einflüsse beim Brennen", *Zement-Kalk-Gips*,
644 Nr. 10, 354-368, 1953
- 645 [4] J. Wuhler: "Wissenschaftliche und verfahrenstechnische Probleme des
646 Kalkbrennens", *Chemie-Ing.-Techn.*, Nr. 1, 19-30, 1958.
- 647 [5] Wolter, S. Luger, G. Schaefer: "Zur Kinetik der Hydratation von Branntkalk",
648 *Zement-Kalk-Gips*, Vol. 57, Nr. 8, 60-68, 2004
- 649 [6] "Lange's handbook of chemistry", 13th Edition, Ed. J.A. Dean, McGraw-Hill, New
650 York, 1985, p. 10-9 (ISBN 0-07-016192-5).

- 651 [7] T. Wagner, D.A. Kulik, F.F. Hingerl, S.V. Dmytrievava: "Gem-selector
652 geochemical modelling package: TSolMod library and data interface for
653 multicomponent phase models", *Can. Mineral.* 50 (2012) 1173–1195.
- 654 [8] D.A. Kulik, T. Wagner, S.V. Dmytrieva, G. Kosakowski, F.F. Hingerl, K.V.
655 Chudnenko, et al.: "GEM-Selector geochemical modelling package: revised algorithm
656 and GEMS3K numerical kernel for coupled simulation codes", *Comput.Geosci.* 17
657 (2013) 1–24.
- 658 [9] W. Hummel, U. Berner, E. Curti, F.J. Pearson, T. Thoenen: "Nagra/PSI chemical
659 thermodynamic data base 01/01", *Radiochim. Acta* (2002) 805–813.
- 660 [10]
661 [https://chem.libretexts.org/Core/Physical_and_Theoretical_Chemistry/Acids_and_](https://chem.libretexts.org/Core/Physical_and_Theoretical_Chemistry/Acids_and_Bases/Acids_and_Bases_in_Aqueous_Solutions/The_pH_Scale/Temperature_Dependence_of_the_pH_of_pure_Water)
662 [Bases/Acids_and_Bases_in_Aqueous_Solutions/The_pH_Scale/Temperature_Depe](https://chem.libretexts.org/Core/Physical_and_Theoretical_Chemistry/Acids_and_Bases/Acids_and_Bases_in_Aqueous_Solutions/The_pH_Scale/Temperature_Dependence_of_the_pH_of_pure_Water)
663 [ndence_of_the_pH_of_pure_Water](https://chem.libretexts.org/Core/Physical_and_Theoretical_Chemistry/Acids_and_Bases/Acids_and_Bases_in_Aqueous_Solutions/The_pH_Scale/Temperature_Dependence_of_the_pH_of_pure_Water)
- 664 [11] "Aquatic Chemistry - Chemical Equilibria and Rates in Natural Waters", Eds. W.
665 Stumm and J.J. Morgan, 3rd Edition, John Wiley & Sons, Inc., New York, 1996, pp.
666 157-163.
- 667 [12] www.engineeringtoolbox.com/gases-solubility-water-d_1148.html
- 668 [13] <http://www.aqion.de/site/191>
- 669 [14] J. Duchesne and E.J. Reardon: "Measurement and prediction of portlandite
670 solubility in alkali solutions", *Cem. Concr. Res.* 25 (1995) 1043-1053.
- 671 [15] J. Johnston and C. Grove, *J. Amer. Soc.*, 53 (1931) 3976
- 672 [16] L.B. Yeatts and W.L. Marshall, *J. Phys. Chem.* 71 (1967) 2641
- 673 [17] Justnes, H., Kim, M.-O., Ng, S, and Qian, X.: "Methodology of Calculating Required
674 Chloride Diffusion Coefficient for Intended Service Life as Function of Concrete Cover
675 in Reinforced Marine Structures", *Cement and Concrete Composites*, Vol. 73, October
676 2016, pp. 316-323.
- 677 [18] *Handbook of Chemistry and Physics*, 71st Edition 1990-1991, Ed. David R. Lide,
678 CRC press, p. 4-77.
- 679 [19] A, Ramsay, K. Gill, A. Morrison and N. Mac Nair: "Hydrated lime application by
680 the PEI aquaculture industry", Technical report #253, Prince Edvard Island (PEI)
681 Department of Fisheries, Aquaculture and Rural Development (DFARD), Canada,
682 August 2014, 28 pp.
- 683 [20] Garmo, Ø., With Fagerli, C., Segtnan, O.A.: «Surveillance of pH during dosing of
684 burnt lime in the Slettnes fjord» (in Norwegian), NIVA memo 1587/17, 19-12-2017.